Characterization of Glioblastoma Cancer Stem Cells Sorted by Sedimentation Field-Flow Fractionation Using an Ultrahigh-Frequency Range Dielectrophoresis Biosensor

Tarek Saydé, Rémi Manczak, Sofiane Saada, Gaelle Bégaud, Barbara Bessette, Gaetane Lespes, Philippe Le Coustumer, Karen Gaudin, Claire Dalmay, Arnaud Pothier, et al.

Characterization of Glioblastoma Cancer Stem Cells sorted by Sedimentation Field-Flow Fractionation, using Ultra High Frequency range Dielectrophoresis biosensor.

Journal:	*Analytical Chemistry*
Manuscript ID	ac-2021-024665.R1
Manuscript Type:	Article
Date Submitted by the Author:	n/a
Complete List of Authors:	Sayde, Tarek; Universite de Limoges, Lab Chimie Analytique; Université de Bordeaux, INSERM U1212, UMR CNRS 5320 Manczak, Rémi; Université de Limoges, XLIM Saada, Sofiane; Universite de Limoges, EA 3842 Captur Bégaud, Gaëlle; Universite de Limoges, Lab Chimie Analytique/ EA 3842 Captur Bessette, Barbara; Universite de Limoges, EA 3842 Captur Lespes, Gaëtane; UPPA -IPREM, LCABIE Le Coustumer, Philippe; Université de Bordeaux, UFR STM, OASU Gaudin, Karen; Université de Bordeaux, INSERM U1212, UMR CNRS 5320 Dalmay, Claire; Université de Limoges, XLIM Arnaud, Pothier; Université de Limoges, XLIM Lalloué, Fabrice; Universite de Limoges, EA 3842 Captur Battu, Serge; Universite de Limoges, Lab Chimie Analytique / EA 3842

Characterization of Glioblastoma cancer stem cells sorted by Sedimentation field-flow fractionation, using Ultra High Frequency range Dielectrophoresis biosensor.

Tarek Saydé[1,2], Rémi Manczak[3], Sofiane Saada[1], Gaelle Bégaud[1], Barbara Bessette[1], Gaëtane Lespes[4], Philippe Le Coustumer[5], Karen Gaudin[2], Claire Dalmay[3], Arnaud Pothier[3], Fabrice Lalloué[1], Serge Battu[1*]

1. EA3842-CAPTuR, GEIST, Faculté de Médecine, Université de Limoges, 2 rue du Dr Marcland, 87025 Limoges, France
2. ARNA, INSERM U1212, UMR CNRS 5320, Université de Bordeaux, 146 rue Léo Saignat, 33076 Bordeaux, France
3. XLIM-UMR CNRS 7252, Université de Limoges, Limoges, France, 123, avenue Albert Thomas - 87060 LIMOGES CEDEX
4. CNRS, Institut des Sciences Analytiques et de Physico-Chimie pour l'Environnement et les Matériaux (IPREM), UMR 5254, Université de Pau et des Pays de l'Adour (E2S/UPPA), 2 Avenue Pierre Angot, 64053 Pau, France
5. Bordeaux Imaging Center, UMS 3420 CNRS-INSERM, Université de Bordeaux, , 146 rue Léo Saignat, 33076 Bordeaux, France

✉ Corresponding author: serge.battu@unilim.fr

Abstract

Cancer Stem Cells (CSC) appear to be an essential target for cancer therapies, in particular in brain tumors such as Glioblastoma. Nevertheless, their isolation is made difficult by their low content in culture or tumors (< 5% of the tumor mass), and is essentially based on the use of fluorescent or magnetic labeling techniques, increasing the risk of differentiation induction. The use of label-free separation methods such as sedimentation field flow fractionation (SdFFF) is promising, but it becomes necessary to consider a coupling with a detection and characterization method for future identification and purification of CSCs from patient-derived tumors. In this study we demonstrate for the first time the capability of using an Ultra High Frequency range Dielectrophoresis (UHF-DEP) fluidic biosensor as a detector. This implies an important methodological adaptation of SdFFF cell sorting by the use of a new compatible carrier liquid DEP buffer (DEP-B). After SdFFF sorting, subpopulation derived from U87-MG and LN18 cells lines, undergo biological characterization, demonstrating that by using DEP-B as a carrier liquid, we sorted by SdFFF subpopulations with specific differentiation characteristics: F1 = differentiated cells / F2= CSCs. These sub-populations presenting high frequency crossover values similar to those measured for standard differentiated (around 110 MHz) and CSC (around 80 MHz) populations. This coupling appeared as a promising solution for the development of an online integration of these two complementary label-free separation/detection technologies.

Introduction

Cancer stem cells (CSCs) are a key point and rare cell type found within a solid tumor, they constitute 1 to 5% of the cells harboring the tumor niche[1]. CSCs are involved in three key processes that control tumor development. [2] First, it has been proven that CSCs can be involved in the growth and development of a tumor mass, due to their multipotency and self-renewal properties that mean the capacity to generate copies of themselves while simultaneously producing different types of differentiated cells.[3, 4] Second, CSCs are also involved in metastatic dissemination. They are able to revert to an epithelial phenotype and thus promote tumor dissemination and metastasis in order to colonize distant organs.[5] Third, CSCs are known to be quiescent, a feature that helps them avert death caused by chemotherapy and radiotherapy.[6] This explain the fact that after initial reduction of the size of the tumor mass, cancer could be regenerated giving rise to relapses.[7, 8] CSCs are present in numerous solid tumors such as Glioblastoma (GBM)[9] and are responsible for tumoral heterogeneity due to their stemness properties.[7] Since CSCs play a key role in tumor initiation, invasion, metastasis and most importantly therapeutic resistance and therapy failure.[1-6], the design and development of new CSC-targeted therapies are of prime importance.[7, 10] Thus, the CSC isolation is crucial for evaluating new therapeutic strategies. However, their characterization and isolation are still limited due to the small percentage of CSCs in the tumor niche or in the cell lines as well as their high plasticity.[10, 11]

Classical approaches in order to characterize CSCs are phenotypic based on membrane markers expression such as CD133[12] and CD44[13], intracellular or intranuclear markers expression such as Sox2[14], Nanog[15] and Oct4[16] They can also be functional like colony forming assays and orthotopics xenograft model on immunosuppresed mice.[17] Because of their plasticity, CSCs are often identified using more than one marker.[18] However, phenotypic changes take place often because of this reversible aspect due to their stemness features; promoting therefore a continuous change in the expression of CSC markers.[19] For example, CD133 was focused on as a major Glioblastoma CSC marker to the point where if a cell is CD133+, it is automatically considered as a CSC.[20] Other studies have proven that

Glioblastoma CSCs are found to be CD133- but positive for other markers like Oct4 and Nanog, hence the need for a pool of markers in order to track down CSCs in a certain cell line.[21] Cell-sorting technologies such as fluorescence activated cell sorting (FACS) and magnetic-activated cell sorting (MACS) are mainly based on these markers to purify specific CSC subpopulations. However, the need of cellular labeling can induce functional changes consequently altering their stemness.[1]

In that way, label-free methods that ensure limited cellular changes in CSCs could be used. One of the most interesting label-free cell sorting methods is the now well-known sedimentation field-flow fractionation (SdFFF) technique.[22-24]. The SdFFF is a gentle and noninvasive technique.[22] The advantage that the SdFFF holds over other sorting techniques is the lack of need of immunolabeling.[22, 25, 26] It relies on cell biophysical properties: size, density and rigidity. The cells are subjected in an empty ribbon-like separation channel (no stationary phase) to two types of forces (1) hydrodynamic lift forces generated by flowing a carrier liquid through the channel and (2) an external field applied perpendicularly to the flow direction.[22, 23, 27] Cells are then eluted under the “Hyperlayer” elution mode, a size/density driven separation mechanism; that ensure a drastic limitation of cell-solid panel interactions.

The end-goal of our work is to investigate the implementation of a label-free method to isolate and characterize CSCs simultaneously, serving as a diagnostic and prognostic approach, based on SdFFF cell sorting. Nevertheless, to perform both cell sorting and population characterization, there is not yet a hyphenated detector like what exists for the asymmetric flow-field flow fractionation (AF4) and multi-angle light scattring (MALS) for entities at a nanoscale.[28-30] Hence, after SdFFF cell sorting; the sub-populations of cells undergo offline biological characterizations. Even though they are effective for routine preparation of CSC from cell line and primary cell culture[23]; they are cost and time consuming, and not adaptated for CSC isolated from highly variable and heterogeneous population for example patient derived tumor sample. To overcome this limitation, a hyphenation of the SdFFF with a label-free based biosensor as a post-sorting online characterizing detector was investigated.

A first step of the development of this solution was previously published[23], that consisted of a combination approach of the SdFFF with a microwave dielectric spectroscopy technique. The latter is based on resonance disturbance principles, corresponding to the microwave range of the electromagnetic spectrum, and permits characterization of cell contents and a mean to discriminate and analyze cells. This technique discriminate between different subpopulations having opposite differentiation status by relying on their intrinsic intracellular dielectric permittivity.[23] While SdFFF combined with a dielectric spectroscope proved its potential to sort and characterize subpopulations of Glioblastoma cell lines, this approach's major limitation resides in the need of fixating cells before introducing them individually between electrodes in a dry non-fluidic system.[23] Therefore, the investigated dead cells can no longer be used in further analysis.

This the reason why we aim to improve the post SdFFF characterization on living cells, by combining SdFFF with a new Ultra High Frequency range Dielectrophoresis (UHF-DEP) biosensor.[31] UHF-DEP is a label-free, accurate, fast, and low-cost characterization method that uses the principles of polarization (in ultra high frequency range from 50 MHz up to 600 MHz) and the motion of living cells in applied electric fields : DEP cell electro-manipulation inside a microfluidic device.[31] UHF-DEP characterization brings information about individual cell cytoplasm content own physical property (dielectric), without lyse nor implied denaturation. The DEP buffer (DEP-B) used as a carrier liquid for the UHF-DEP is osmotic sucrose based survival buffer. Previously, two sub-populations of Glioblastoma cell lines, one enriched with CSCs by cultivating the cells in a gold standard define medium (DM) and another cultivated in a normal medium (NM) with high percentage of differentiated cells, were discriminated using the UHF-DEP.[31] The population with the high percentage of CSCs (in DM) exhibited lower high frequency crossover (HFC) values than that of a population with high percentage of differentiated cells (in NM). In this manner, we now consider the HFC or electromagnetic signature (EM) as a marker for CSCs discrimination, confirming the UHF-DEP biosensor's potential.[31]

The foreseen target of this work is an online hyphenation of SdFFF and the biosensor. In this paper, we have to prove, via an offline coupling, the compliance between cell sorting by SdFFF and the characterization by UHF-DEP. In view of a future online hyphenation, it was logical to use from this point forward one common carrier liquid for both systems. The choice is made on the buffer compatible with the detector, DEP-B, which implies the validation of the elution conditions by SdFFF with DEP-B as a carrier liquid instead of the usually used phosphate buffer solution (PBS).[23] After cell sorting by SdFFF with this new carrier liquid, cell sub-populations undergo biological characterizations, generating populations enriched or not in CSCs. The HFC values of each sub-population were measured by UHF-DEP by comparison to a gold standard. The HFC values of the SdFFF sub-population enriched in CSCs is similar to the reference population, proving the validity of this approach and the practical application of the future online hyphenation and its clinical relevance in the future.

Materials and methods

Schematic representations of the offline hyphenation of SdFFF and UHF-DEP biosensor are presented in Figure SI-1.

Cell culture: The human glioblastoma cell lines U87-MG and LN18 were purchased from the American Type Culture Collection (ATCC, Manassas, VA, USA) and grown under two conditions: NM (normal medium with fetal bovine serum [FBS]) and DM (define medium [serum-free]). The schematic representation of the experimental conditions is represented in Figure SI-2. The NM and DM compositions are previously described.[23] Cell culture is conducted at a 500.10^3 density rate for 72h for U87-MG and 750.10^3 for 48h for LN18. After culture time, cells are dissociated using versene solution (Thermofisher scientific, France) and centrifuged at 300 g for 5'. Cells are then resuspended in DEP-B, an ion free osmotic medium TRIS buffer-based, composed by a water/sucrose mixture with magnesium chloride (pH: 7.4; conductivity: 26 mS/m) conventionally used for DEP experiments.[31] Cells are then counted using trypan blue (Sigma) exclusion and Malassez cell counting chamber. Volume is adjusted to obtain $2,5.10^6$ cells per 1000 µL.

SdFFF device and cell elution conditions: The SdFFF separation device used in this study was previously described.[23] Optimal elution conditions were as follows: flow injection through the accumulation wall of a 100 µL U87-MG and LN18 cell suspension (2×10^6 cells/mL). Flow rate: 1.0 mL/min. Carrier liquid: sterile DEP-B, pH 7.4 and conductivity 24 mS/m. External multigravitational field strength: 15 g for U87-MG (312.5 rpm) and 25 g for LN18 (402.5 rpm) ± 0.2 g. Time dependent fraction collection: **F1**: 2'40'' to 4'20" for U87-MG; and 2'30'' to 4'45'' for LN18. **F2**: 5'55'' to 8'00" for U87-MG; and 8'30" to 12'00" for LN18. **TP** (total peak: fractions constituting the collection of the total eluted population (except the void volume, see figure 2) as an internal control): 2'00" to 8'00" for U87-MG; from 2'00" to 12'00" for LN18. The **crude** population constitute the remaining unsorted cells suspension is used as the external control population. In order to obtain a sufficient quantity of cells for further analysis and subculture, consecutive (10 - 12 injections) SdFFF fraction collections were performed.

Tools and methodology for cell crossover frequency measurement: In this study we aim to characterize sub-populations of GBM cell lines subsequent to their sorting, by measuring their cross-over frequencies in the ultra-high frequency range. The measurement process was fully described previously.[31] It consists in submitting individual cell to a High Frequency electric field and monitoring under microscope, while tuning by signal frequency, the induced cell motion. When cells are submitted to negative DEP forces, they are repelled, to the contrary they are attracted by a positive DEP force. When the electric field frequency reaches the cell crossover frequency, the DEP force become null, and it can be measured from the optically observable cell change of motion behavior.

For the present study, a dedicated microfluidic chip has been used based on aluminum passivated microelectrodes forming a 90° quadrupole sensor (Figure 1 A). This sensor has been implemented on *@IHP Innovations for High Performance Microelectronics* BiCMOS silicon technology substrate, diced into cm² chip and packaged with a Polydiméthylsiloxane (PDMS) cover to form a 200 µm wide and 40 µm high microfluidic channel above the sensor (Figure 1 C). As shown in figure 1, led experiments were done using a 40×40µm gap electrodes design that combines a pair of thick electrodes (9 µm, see figure 1A and SI-1B), that crossed the microfluidic channel width, with another pair of thin electrodes (0.45 µm, Figure 1A) implemented in the middle of the channel where most of the cells flow (Figure 1C). Such design allows generating an electric field gradient configuration presenting a very localized low magnitude field spot in the middle of the structure to the contrary with high magnitude barriers surrounded electrode edges (Figure 1B simulated electric field insert). Hence properly biasing the left and right electrodes with a high frequency signal, whereas top and bottom ones are grounded, it is hence possible to form an efficient electrical trap to catch biological cells flowing in the main central channel part (Figure SI-1B). The sensor is biasing though 50 ohm (10µm wide) microstrip lines implemented under the PDMS cap until the chip edges thanks to an microwave signal generator (R&S®SMB100A) associated with a wide band amplificator (Bonn Elecktrik BLWA 110-5M) able to generate high purity continuous wave signal with magntitude up to 10Vpp . For current experiment the typically magnitude of the applied voltage ranges between 2 and 4 Vpp.

Cellular characterizations

A complete description of the phenotypical and functional characterization of cell subpopulations is shown in the Supporting Information (see SI-1 and SI-2).

Analysis of cell size using a Coulter counter: Cell size means of different populations are measured subsequent to SdFFF cell sorting.

RTqPCR: mRNA expression levels of CSC markers are evaluated in the different populations.

Soft agar clonogenic assay: a method used to test the ability of the cells to form clones in soft agar for CSCs are known to have high clonogenic properties by comparison to differentiated cells.

DNA cell cycle analysis: a method that most frequently employs flow cytometry to distinguish cells in different phases of the cell cycle: CSCs are known to be quiescent hence in the G1 phase whereas differentiated cells are proliferative and ready to undergo mitosis hence tend to be in the G2 phase.

Statistical Analysis: Statistical analysis were performed on three independent experiments using Prism graphpad. Analysis of variance (ANOVA), t student and Mann-Whitney tests were conducted to compare different conditions. P values of ≤ 0.05 were considered statistically significant.

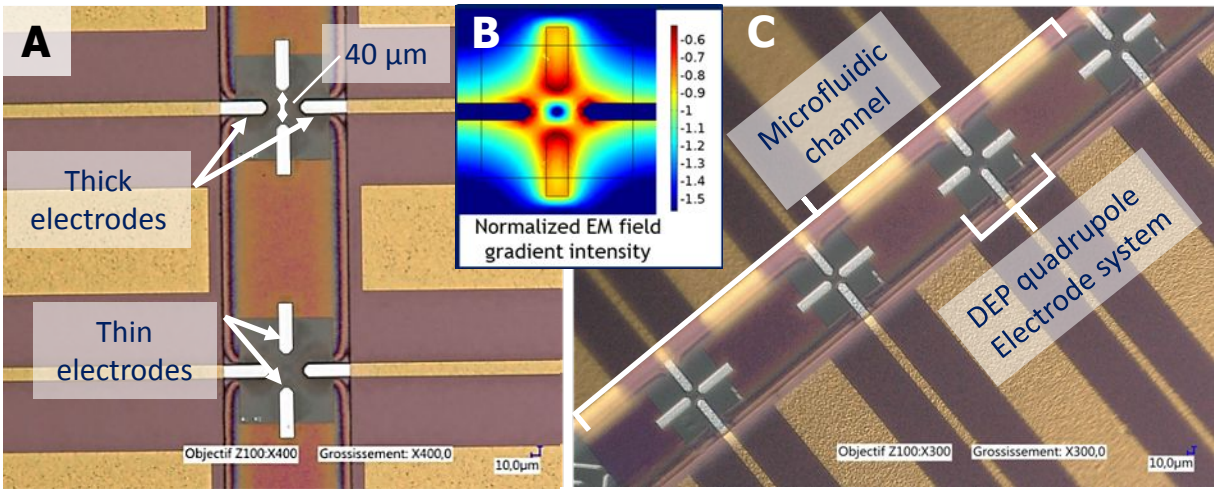

Figure 1. UHF-DEP detetctor: A: Top view of quadrupole electrode sensor used for HFC frequency measurement. Two types of electrodes are present, thin (top and bottom) and thick (left and right), with a gap of 40 µm. **B:** simulated electric field into the Dep quadrupole electrode system. **C:** angle view through the PDMS cap of sensor array under PDMS cap implemented at the bottom of a microfluidic channel.

Results and discussion

Methodological development of SdFFF cell sorting.

SdFFF with DEP-B as a carrier liquid

In the goal of combining SdFFF and UHF-DEP, which are two fluidic devices having each their own carrier liquid, we decided to use the detector compatible carrier liquid, the DEP-B, because UHF-DEP is not operational with PBS due to high content of salt whereas SdFFF could be investigated with either DEP-B or PBS as a carrier liquid.

Nevertheless, the use of DEP-B as carrier liquid for SdFFF, requires a new methodological development and validation step for SdFFF cell sorting. The presence of sucrose (8.5%[31]) in the DEP-B medium leads to an important change in the elution profile of U87-MG and LN18 (Figure. 2), most likely due to the slight change in density (PBS : 1.0034 / DEP : 1.031). A better resolution of cell peak vs. dead volume peak, facilitating fraction collection, was observed (Figure. 2A and 2B). This is particularly true concerning U87-MG compared to previously published fractograms.[23] These profiles also present reproducibility and repeatability with CV< 5% in terms of elution time. Finally, the cell viability throughout the conservation of cells in DEP-B remains higher than that observed in PBS for both cell lines. (see Table SI-1)

The usually described SdFFF elution mode for cells is the “hyperlayer” mode[22, 23, 32, 33] in which subpopulations of cells are focused into a thin layer at an equilibrium position in the channel thickness, depending on their biophysical properties: size and density as first-order parameters, along with shape and rigidity.[24] Hyperlayer elution order is size- and density- dependent: larger and less dense cells are focused in the faster streamlines, and are consequently eluted first. The experimental retention ratio, R_{obs} (void time divided by retention time [t_0 / t_R], measured by the first moment method)[34], was calculated to determine the average velocities and elution modes.

Under our elution conditions (see Material and Methods section), we obtained for both cell lines, fractograms with two (U87-MG) or three (LN-18) (Figure. 2A and 2B) major peaks, the first

corresponding to non-retained species (void volume peak, $R_{obs} \approx 1$), and the second (and third) corresponding specifically to cell subpopulations with $R_{obs} < 1$. (see below)

Hyperlayer elution mode was first determined based on the field and flow rate dependence of R_{obs}.[23, 27, 32, 33] Then, at equivalent flow rates, the increase in field strength focused cells in slower stream lines, increasing retention and decreasing R_{obs}. In that way U87-MG shown a decrease in R_{obs} of 33% by increasing the field from 10 to 20g, and 13% for LN18 by increasing the field from 20 to 30g. This low difference could be explain by the fact that LN18 were eluted with higher field strength.

In hyperlayer elution mode, samples were lifted away from the accumulation wall, limiting harmful cell–surface interactions. By using the following equation[35]

$$s = \frac{R_{obs} \times \omega}{6}$$

in which ω is the channel thickness (175 µm), we calculated the value of **s**, the average distance from the center of the cell to the channel wall,[35] which should be greater than the particle radius **r**, calculated from the mean cell diameter. The mean R_{obs} value calculated for U87-MG is 0.361 ± 0.004, and 0.273 ± 0.004 for LN18, leading respectively to **s** = 10.5 µm and **s** = 8.0 µm. These values appeared greater than the mean radius measured using coulter counter (see materials and methods) on the total peak population which are 8.0 µm for U87-MG and 7.0 µm for LN18.

Finally, the hyperlayer elution mode relies mainly on biophysical properties of the cell such as cell size and density.[22, 23, 27, 32] As described before, bigger and less dense, are eluted in first, whereas smaller and denser cells are eluted last. Subsequent to their sorting and fraction collection (see Material and Methods section), the mean of sub-populations size was investigated using a Coulter Counter. The F1 fraction displayed a significantly higher size mean than that of the F2 fraction with a difference of Δd = 1.9 µm for U87-MG (Figure. 3A) and Δ = 2.7 µm for LN18 (Figure SI-3A). Then according to the results of R_{obs} variation, **s** measurement and size variation, we can assume that cells are eluted under hyperlayer elution using DEP-B as a carrier liquid.

Nevertheless, a major change in the elution parameters, such as changing the mobile requires a series of biological characterization for both cell lines in order to validate the SdFFF's efficiency to sort CSCs.

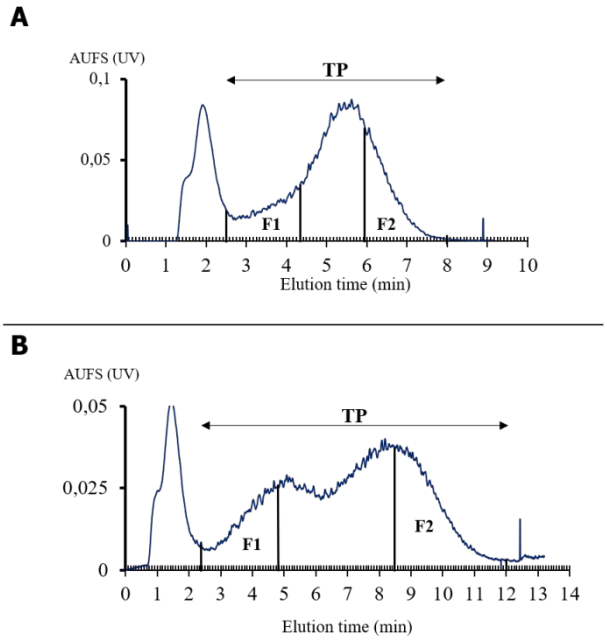

Figure 2. SdFFF fractograms of cells cultured in NM prior to sorting: (A) U87-MG cell line, carrier liquid: sterile DEP-B; (B) LN18 cell line, carrier liquid: sterile DEP-B. Elution conditions flow and field 1.0 mL/min and 15g or 25g for U87-MG and LN18 respectively. Time dependent fraction collections: see materials and methods section.

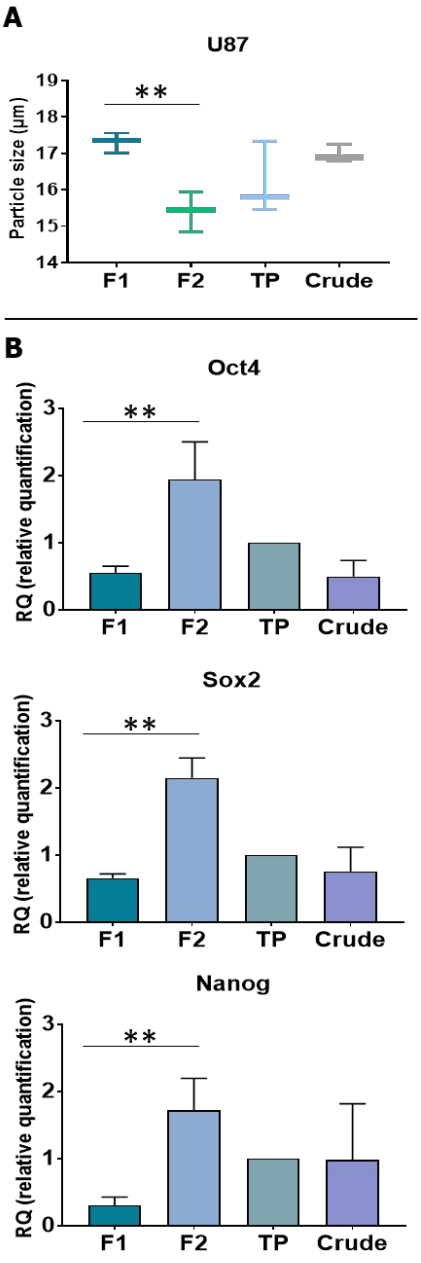

Figure 3. Phenotypical characterizations of the different sub-populations of U87-MG sorted by SdFFF (A) Biophysical proprety: cell size analysis by coulter counter of post SdFFF populations (F1, F2, TP and crude) (B) Comparative analysis of gene expression of three CSCs markers: Oct-4, Sox2 and Nanog, in U87-MG cell line, of the post SdFFF populations (F1, F2, TP and Crude), measured by Real Time quantitative PCR (Polymerase Chain Reaction) and normalized compared to TP. (see SI-1) The p value was determined using t student test or Mann-Whitney test. ** represents p value < 0.001.

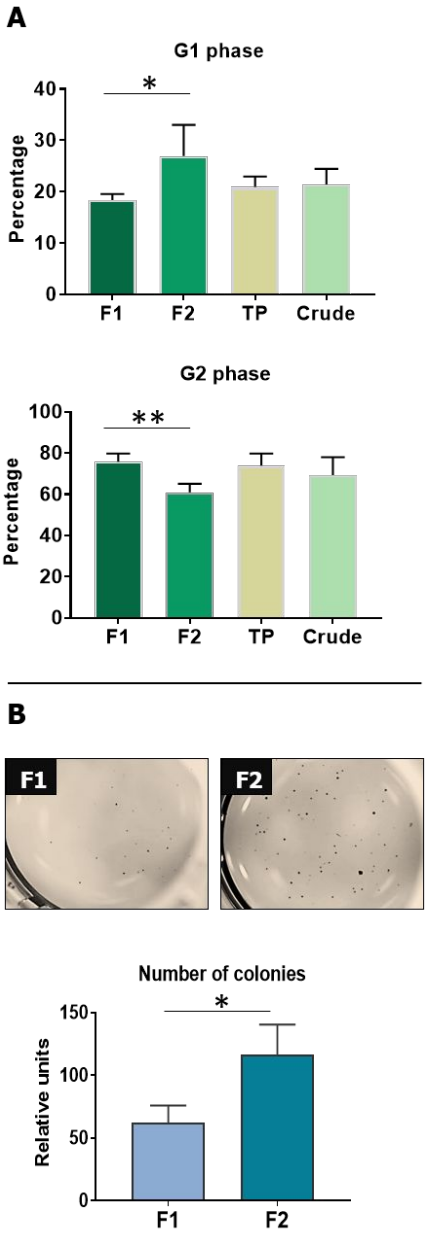

Figure 4. Functional characterizations of the different sub-populations of U87-MG sorted by SdFFF (A) Cell cycle analysis by DNA content measurement: showing that CSCs (F2), the quiescent cells, are more likely found in the G1 phase, vice versa to differentiated cells. (B) Soft agar assay for colony formation examination evaluating the sub-populations capacity to form clones when cultured in soft agar (see SI-2) The p value was determined using t student test. ** represents p value < 0.001 and * represents p value < 0.05

Phenotypical characterization

CSCs plasticity results in an intratumoral heterogeneity observed in solid tumors such as Glioblastoma[36]. For this matter, evaluating the expression of one marker is not enough to conclude on stemness properties, but a pool of CSCs markers is mandatory. Many markers have been identified to be overexpressed in CSCs such as the transcription factors Sox2[14], Nanog[15] and Oct4[16, 23]. This increase in expression is oftenly evaluated at a transcriptomic levels. Differential analysis of CSCs mRNA expression levels was assessed in the sub-populations F1 and F2 by RTqPCR for U87-MG and LN18 cell lines. All three CSCs markers (Oct4, Sox2 and Nanog) for U87-MG are significantly overexpressed in F2 enriched in undifferentiated cells compared to F1 enriched in differentiated cells: 3.5 folds higher in F2 than F1 for Oct4, 3.2 folds higher in F2 than F1 for Sox2 and 5.6 folds higher in F2 than F1 for Nanog (Figure. 3B, see Figure SI-3B for LN18). The overexpression of CSC markers confirms that F2 cell subpopulation is efficiently enriched in CSC.

CSCs tend to remain quiescent within the tumor niche so they can maintain their multipotency, consequently the main source supplying tumor growth.[37, 38] For this matter, CSCs are often found at the G1 phase of the DNA cell cycle, also known as the quiescence phase. Whereas differentiated cells, the more mature and ready to proliferate, are found at the G2 phase, also known as the growth phase.[39] Our DNA cell cycle analysis showed a higher tendency for the U87-MG F1 sub-population to be in the G2 phase of the cell cycle, while the U87-MG F2 sub-population enriched in CSCs is found to be in the G1 phase (Figure. 4A, see Figure SI-3C for LN18). This confirms that we have managed to isolate and enrich a sub-populaton of cells having high stemness characteristics as revealed transcriptomic and cell cycle analysis.

Functional characterization

CSCs have the capability to form an important quantity of colonies due to their self-renewal properties.[17] Soft agar colony formation assay is considered as one of the most rigorous and effective techniques for evaluating this capability *in vitro* [40] and characterizing stemness properties of cells.[41]

Our soft agar assay shows that the U87-MG F2 sub-population managed to form a high number of colonies within 30 days of culture in soft agar, therefore exhibiting a stem-like behavior unlike U87-MG F1 (Figure. 4B, see Figure SI-3D for LN18). This test validates the functional aspect of the CSCs population.

This series of biological characterization proves that, after cell line culture in NM, the F2 sub-population, consists of a population of cells enriched in CSCs, whereas the F1 sub-population is enriched in differentiated cells for both U87-MG and LN18 cell lines. Therefore, the SdFFF is validated as a cell sorting label free method using DEP-B as a carrier liquid instead of PBS.

Cell characterization with UHF-DEP biosensor subsequent to their sorting

Crossover frequencies of GBM cells cultured in NM before SdFFF

The SdFFF technique has proven its potential to isolate a population enriched in CSCs using the DEP-B as a carrier liquid. In order to validate the possibility of an association between SdFFF and UHF-DEP, the sub-populations (F1, F2), TP and crude of the two GBM cell lines, U87-MG and LN18, were characterized by measuring their HFC values with UHF-DEP. The HFC considered, corresponds to the frequency at which the trapped cell begins to move away from the center of the quadrupole electrodes. (see figure SI-2 for abbreviations and experimental conditions)

In previous work, it has been demonstrated that the more the population is enriched in CSCs, the lower the HFC values of the cells are, by comparison to differentiated cells cultured.[31] In a same way, we cultured in this study the two glioblatoma cell lines (U87-MG/LN18) in normal medium (NM) and in the define medium (DM) known to enrich the population in CSC.

First, the sub-populations of U87-MG and LN18 cultured in NM sorted by SdFFF with DEP-B were characterized by UHF-DEP biosensor. As shown in Figure 5A and Table SI-2, for U87-MG, the median HFC value of the F1 sub-population (U87-MG F1 NM) is similar to that of the unsorted cells cultured in NM (U87-MG NM) (respectively 103 MHz and 111 MHz). Whereas the median HFC value of the F2 sub-population (U87-MG F2 NM) is similar to that of the unsorted cells cultured in DM (U87-MG DM)

(respectively 81 MHz and 85 MHz). Similar results were observed in Figure SI-4 and Table SI-2, with LN18 where the median HFC value of the F1 sub-population (LN18 F1 NM) is similar to that of the unsorted cells cultured in NM (LN18 NM) (respectively 109 MHz and 119 MHz). Whereas the median HFC value of the F2 sub-population (LN18 F2 NM) is similar to that of the unsorted cells cultured in DM (LN18 DM) (respectively 74 MHz and 77 MHz).

This finding indicates that the sub-populations F1 and F2 sorted by SdFFF with DEP-B as a carrier liquid, exhibited crossover frequencies respective of differentiated cells for F1 and CSCs for F2. These results obtained with an offline approach, validate the relevance of an online hyphenation of SdFFF as a cell sorting technique and UHF-DEP as a post sorting detector.

Thus far, all of these characterizations have been done on cells cultured in NM prior to their sorting by SdFFF with DEP-B. However, as previously done[23], we wanted to examine the possibility of purifying even further the population of CSCs, by cultivating the cells in DM, sorting the population with SdFFF and finally characterizing the generated sub-populations by UHF-DEP. Both cell lines were cultured in DM for 6 days, and then sorted by SdFFF with DEP-B (see figure SI-5)

The median HFC value of the F1 sub-population post DM culture (U87-MG F1 DM) is 81.5 MHz and of the F2 sub-population post DM culture (U87-MG F2 DM) is 73 MHz. Both HFC values are very close to that of the previously measured U87-MG F2 NM population (81 MHz) (Figure 5B, see Table SI-2). This result was expected because even before cell sorting, the entire population was highly enriched in CSCs because of the DM, therefore both sub-populations are equally enriched in CSCs. Similar results were obtained with LN18 where the median HFC value of LN18 F1 DM is 80 MHz and LN18 F2 DM is 72 MHz, similar to that of the unsorted cells cultured in DM (LN18- DM) with a median of 77 MHz (see Figure SI-4 and Table SI-2).

These results indicate that the SdFFF has successfully managed to purify to the highest extent a sub-population enriched in CSCs. It conveys a population sorted by SdFFF and characterized by UHF-biosensor without the need of a DM for CSCs enrichment. In addition, the NM conserves the heterogeneity of the CSCs population. The clear advantage that was observed is that the cells cultured

in NM maintain a high viability rate (95% for U87-MG and 93% for LN18) after SdFFF cell sorting with UHF-B, whereas cells cultured in DM before SdFFF are subjected to highly stressful conditions that result in a significative decrease in cell viability (60% for U87-MG and 40% for LN18). The preservation of this high viability of CSCs after normal elution conditions by SdFFF, opens the door to a wide variety of applications, most importantly the design of diagnostic approaches, targeted therapies and a deeper understanding of CSCs in general.

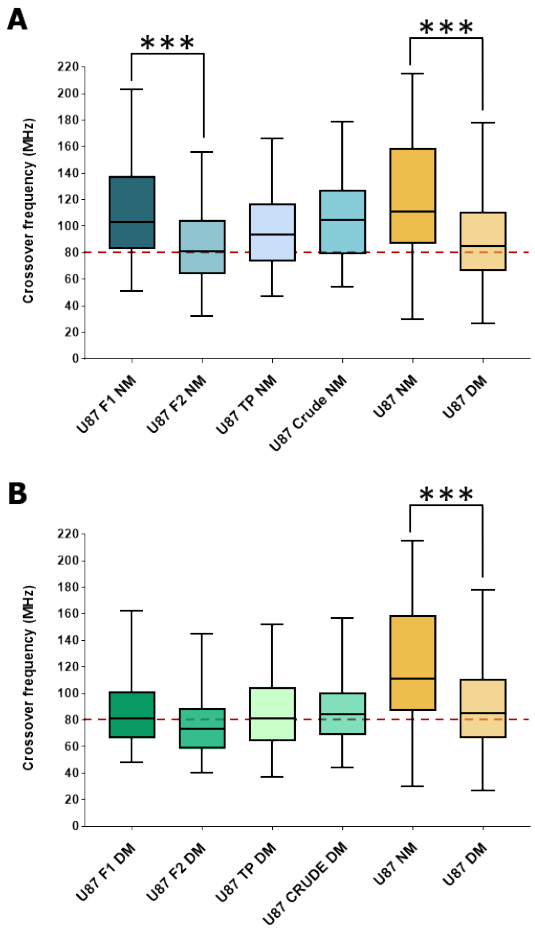

Figure 5: Graphic box plots representation of the high frequency crossover values of U87-MG cells (A) cultured in NM and sorted by SdFFF (U87 F1 NM and U87 F2 NM); (B) cultured in DM and sorted by SdFFF (U87 F1 DM and U87 F2 DM). Cells cultured in NM and DM without sorting (U87 NM and U87 DM). The red threshold represents the median of U87-MG F2 NM. The p value was determined using One-way ANOVA test. *** represents p value < 0.0001.

Conclusion

Unlike other types of FFF separation techniques, the SdFFF used as a cell sorter lacks an online label-free characterization. In previous studies, an association between SdFFF and a label-free detector has been investigated.[23] This approach failed to maintain cell viability after characterization. For this matter, in this study, we aimed to investigate a possible association between SdFFF and a microfluidic label-free biosensor in the ultra-high frequency range. Both SdFFF and UHF-DEP biosensor have individually proven their potential to respectively sort and characterize cells without labeling while maintaining high cell viability. First, this coupling required a compatibility investigation between both techniques that revealed the need of a methodological development of SdFFF in order to adapt to the detector. By unifying the carrier liquid for a DEP-B compatible medium, our work has shown that the SdFFF was capable of sorting two sub-populations of glioblastoma cell lines having opposite states of differentiation. All the physical and biological parameters studied (phenotypical and functional) proved the enrichment of CSCs in the F2. The high frequency crossover values of the sub-populations subsequent to FFF sorting showed a unique HFC to each population similar to that of gold standard measurements. This study aims to prove the feasibility and re-adaptation of the separation method to be compatible with the detection method. These two label-free techniques allowed cell separation on the basis of orthogonal properties: size, density, shape, rigidity for FFF; and the dielectrophoretic properties for UHF-DEP, for the diagnostic management of complex tumor populations originating from the patient. In the context of an application using patient derived cells, it is practically impossible to use a gold standard medium such as the DM to enrich the population in CSCs. Therefore, an online device SdFFF/UHF-DEP is inevitable for these sorts of applications and analysis. An ongoing development consists of determining the setting up of one single fast, low cost and effective tool that enhances the evaluation of CSCs in tumors opening the door to novel diagnostic, prognostic and theranostics approaches.

Notes

Corresponding author: Serge Battu, serge.battu@unilim.fr

The authors declare no competing financial interest.

Supporting Information

SI contains the following: description of phenotypical and functional characterization of cell subpopulations / figures for schematic representations of both technique's offline coupling, for experimental conditions of cell culture / figures for phenotypical and functional characterization of LN18 cell line/ fractograms in DM conditions, cell viability and finally a table with the values of HFC.

Acknowledgments

This study was supported by the European Project No. SUMCASTEC (Horizon 2020 Research and Innovation Programme under Grant Agreement No. 737164) and ''Région Nouvelle Aquitaine'' (2018-1R10128).

References

1. Cheray, M.; Begaud, G.; Deluche, E.; Nivet, A.; Battu, S.; Lalloue, F.; Verdier, M.; Bessette, B., Cancer Stem-Like Cells in Glioblastoma. In *Glioblastoma*, 2017/12/19 ed.; De Vleeschouwer, S., Ed. Codon Publications: Brisbane, 2017.
2. Dawood, S.; Austin, L.; Cristofanilli, M. Cancer stem cells: implications for cancer therapy. *Oncology* **2014,** *28* (12), 1101-7, 1110.
3. Batlle, E.; Clevers, H. Cancer stem cells revisited. *Nat. Med.* **2017,** *23* (10), 1124-1134.
4. Matsui, W. H. Cancer stem cell signaling pathways. *Medicine* **2016,** *95* (1 Suppl 1), S8-S19.
5. Chang, J. C. Cancer stem cells: Role in tumor growth, recurrence, metastasis, and treatment resistance. *Medicine* **2016,** *95* (1 Suppl 1), S20-S25.
6. Luo, M.; Li, J. F.; Yang, Q.; Zhang, K.; Wang, Z. W.; Zheng, S.; Zhou, J. J. Stem cell quiescence and its clinical relevance. *World J Stem Cells* **2020,** *12* (11), 1307-1326.
7. Nassar, D.; Blanpain, C. Cancer Stem Cells: Basic Concepts and Therapeutic Implications. *Annu Rev Pathol* **2016,** *11*, 47-76.
8. Pan, Y.; Ma, S.; Cao, K.; Zhou, S.; Zhao, A.; Li, M.; Qian, F.; Zhu, C. Therapeutic approaches targeting cancer stem cells. *J Cancer Res Ther* **2018,** *14* (7), 1469-1475.
9. Singh, S. K.; Hawkins, C.; Clarke, I. D.; Squire, J. A.; Bayani, J.; Hide, T.; Henkelman, R. M.; Cusimano, M. D.; Dirks, P. B. Identification of human brain tumour initiating cells. *Nature* **2004,** *432* (7015), 396-401.
10. Clevers, H. The cancer stem cell: premises, promises and challenges. *Nat Med* **2011,** *17* (3), 313-9.
11. Kuşoğlu, A.; Biray Avcı, Ç. Cancer stem cells: A brief review of the current status. *Gene* **2019,** *681*, 80-85.
12. Liou, G. Y. CD133 as a regulator of cancer metastasis through the cancer stem cells. *Int J Biochem Cell Biol* **2019,** *106*, 1-7.
13. Yan, Y.; Zuo, X.; Wei, D. Concise Review: Emerging Role of CD44 in Cancer Stem Cells: A Promising Biomarker and Therapeutic Target. *Stem Cells Transl Med* **2015,** *4* (9), 1033-43.
14. Zhu, F.; Qian, W.; Zhang, H.; Liang, Y.; Wu, M.; Zhang, Y.; Zhang, X.; Gao, Q.; Li, Y. SOX2 Is a Marker for Stem-like Tumor Cells in Bladder Cancer. *Stem Cell Reports* **2017,** *9* (2), 429-437.
15. Buczek, M. E.; Reeder, S. P.; Regad, T. Identification and Isolation of Cancer Stem Cells Using NANOG-EGFP Reporter System. *Methods Mol Biol* **2018,** *1692*, 139-148.
16. Mohiuddin, I. S.; Wei, S. J.; Kang, M. H. Role of OCT4 in cancer stem-like cells and chemotherapy resistance. *Biochim Biophys Acta Mol Basis Dis* **2020,** *1866* (4), 165432.

17. Rajendran, V.; Jain, M. V. In Vitro Tumorigenic Assay: Colony Forming Assay for Cancer Stem Cells. *Methods Mol Biol* **2018,** *1692*, 89-95.

18. Vlashi, E.; Pajonk, F. Cancer stem cells, cancer cell plasticity and radiation therapy. *Semin Cancer Biol* **2015,** *31*, 28-35.

19. Yakisich, J. S.; Azad, N.; Kaushik, V.; Iyer, A. K. V. Cancer Cell Plasticity: Rapid Reversal of Chemosensitivity and Expression of Stemness Markers in Lung and Breast Cancer Tumorspheres. *J Cell Physiol* **2017,** *232* (9), 2280-2286.

20. Schmohl, J. U.; Vallera, D. A. CD133, Selectively Targeting the Root of Cancer. *Toxins (Basel)* **2016,** *8* (6).

21. Beier, C. P.; Beier, D. CD133 negative cancer stem cells in glioblastoma. *Front Biosci (Elite Ed)* **2011,** *3*, 701-10.

22. Mélin, C.; Perraud, A.; Akil, H.; Jauberteau, M. O.; Cardot, P.; Mathonnet, M.; Battu, S. Cancer Stem Cell Sorting from Colorectal Cancer Cell Lines by Sedimentation Field Flow Fractionation. *Anal. Chem.* **2012,** *84* (3), 1549-1556.

23. Lacroix, A.; Deluche, E.; Zhang, L. Y.; Dalmay, C.; Melin, C.; Leroy, J.; Babay, M.; Du Puch, C. M.; Giraud, S.; Bessette, B.; Begaud, G.; Saada, S.; Lautrette, C.; Pothier, A.; Battu, S.; Lalloue, F. A New Label-Free Approach to Glioblastoma Cancer Stem Cell Sorting and Detection. *Anal. Chem.* **2019,** *91* (14), 8948-8957.

24. Faye, P.-A.; Vedrenne, N.; De la Cruz-Morcillo, M. A.; Barrot, C.-C.; Richard, L.; Bourthoumieu, S.; Sturtz, F.; Funalot, B.; Lia, A.-S.; Battu, S. New Method for Sorting Endothelial and Neural Progenitors from Human Induced Pluripotent Stem Cells by Sedimentation Field Flow Fractionation. *Anal. Chem.* **2016,** *88* (13), 6696-6702.

25. Guglielmi, L.; Battu, S.; Le Bert, M.; Faucher, J. L.; Cardot, P. J. P.; Denizot, Y. Mouse embryonic stem cell sorting for the generation of transgenic mice by sedimentation field-flow fractionation. *Anal. Chem.* **2004,** *76*, 1580-1585.

26. Naves, T.; Battu, S.; Jauberteau, M.-O.; Cardot, P. J. P.; Ratinaud, M.-H.; Verdier, M. Autophagic Subpopulation Sorting by Sedimentation Field-Flow Fractionation. *Anal. Chem.* **2012,** *84* (Copyright (C) 2012 American Chemical Society (ACS). All Rights Reserved.), 8748-8755.

27. Mélin, C.; Lacroix, A.; Lalloué, F.; Pothier, A.; Zhang, L. Y.; Perraud, A.; Dalmay, C.; Lautrette, C.; Jauberteau, M. O.; Cardot, P.; Mathonnet, M.; Battu, S. Improved sedimentation field-flow fractionation separation channel for concentrated cellular elution. *J. Chromatogr. A* **2013,** *1302*, 118-124.

28. Bocca, B.; Battistini, B.; Petrucci, F. Silver and gold nanoparticles characterization by SP-ICP-MS and AF4-FFF-MALS-UV-ICP-MS in human samples used for biomonitoring. *Talanta* **2020,** *220*, 121404.

29. Bousse, T.; Shore, D. A.; Goldsmith, C. S.; Hossain, M. J.; Jang, Y.; Davis, C. T.; Donis, R. O.; Stevens, J. Quantitation of influenza virus using field flow fractionation and multi-angle light scattering for quantifying influenza A particles. *J Virol Methods* **2013,** *193* (2), 589-96.

30. González-Espinosa, Y.; Sabagh, B.; Moldenhauer, E.; Clarke, P.; Goycoolea, F. M. Characterisation of chitosan molecular weight distribution by multi-detection asymmetric flow-field flow fractionation (AF4) and SEC. *Int J Biol Macromol* **2019,** *136*, 911-919.

31. Manczak, R.; Saada, S.; Provent, T.; Dalmay, C.; Bessette, B.; Bégaud, G.; Battu, S.; Blondy, P.; Jauberteau, M. O.; Kaynak, C. B.; Kaynak, M.; Palego, C.; Lalloué, F.; Pothier, A. UHF-Dielectrophoresis Crossover Frequency as a New Marker for Discrimination of Glioblastoma Undifferentiated Cells. *IEEE J-ERM* **2019,** *3* (3), 191–198. .

32. Bégaud-Grimaud, G.; Battu, S.; Leger, D. Y.; Cardot, P. J. P., Mammalian Cell Sorting with Sedimentation Field Flow Fractionation. In *Field-Flow Fractionation in Biopolymer Analysis*, Williams, S. K. R.; Caldwell, K. D., Eds. Springer-Verlag: Wien, 2012.

33. Caldwell, K. D.; Cheng, Z. Q.; Hradecky, P.; Giddings, J. C. Separation of human and animal cells by steric field-flow fractionation. *Cell Biophys.* **1984,** *6* (4), 233-251.

34. Williams, P. S.; Lee, S.; Giddings, J. C. Characterization of hydrodynamic lift forces by field-flow fractionation. Inertial and near-wall lift forces. *Chem. Eng. Commun.* **1994,** *130*, 143-166.

35. Chmelik, J. Different elution modes and field programming in gravitational field-flow fractionation; I. A theoretical approach. *J. Chromatogr. A* **1999,** *845* (1-2), 285-291.

36. Thankamony, A. P.; Saxena, K.; Murali, R.; Jolly, M. K.; Nair, R. Cancer Stem Cell Plasticity - A Deadly Deal. *Front Mol Biosci* **2020,** *7*, 79.

37. Hussein, D.; Punjaruk, W.; Storer, L. C.; Shaw, L.; Othman, R.; Peet, A.; Miller, S.; Bandopadhyay, G.; Heath, R.; Kumari, R.; Bowman, K. J.; Braker, P.; Rahman, R.; Jones, G. D.; Watson, S.; Lowe, J.; Kerr, I. D.; Grundy, R. G.; Coyle, B. Pediatric brain tumor cancer stem cells: cell cycle dynamics, DNA repair, and etoposide extrusion. *Neuro Oncol* **2011,** *13* (1), 70-83.

38. Pauklin, S.; Vallier, L. The cell-cycle state of stem cells determines cell fate propensity. *Cell* **2013,** *155* (1), 135-47.

39. Lathia, J. D.; Mack, S. C.; Mulkearns-Hubert, E. E.; Valentim, C. L. L.; Rich, J. N. Cancer stem cells in glioblastoma. *Genes & Development* **2015,** *29* (12), 1203-1217.

40. Borowicz, S.; Van Scoyk, M.; Avasarala, S.; Karuppusamy Rathinam, M. K.; Tauler, J.; Bikkavilli, R. K.; Winn, R. A. The soft agar colony formation assay. *J Vis Exp* **2014,** (92), e51998.

41. Wang, Z.; Zhou, L.; Xiong, Y.; Yu, S.; Li, H.; Fan, J.; Li, F.; Su, Z.; Song, J.; Sun, Q.; Liu, S. S.; Xia, Y.; Zhao, L.; Li, S.; Guo, F.; Huang, P.; Carson, D. A.; Lu, D. Salinomycin exerts anti-colorectal cancer activity by targeting the β-catenin/T-cell factor complex. *Br J Pharmacol* **2019,** *176* (17), 3390-3406.

Table of Contents/Abstract Graphics